



Published in final edited form as:

Macromol Rapid Commun. 2020 June ; 41(11): e2000061. doi:10.1002/marc.202000061.

pH-Responsive Polymers for Improving the Signal-to-Noise Ratio of Hypoxia PET Imaging with [¹⁸F]Fluoromisonidazole

Dr. Jeroen A. C. M. Goos,

Department of Clinical Neuroscience and MedTechLabs, Karolinska Institute, Solna 17177, Sweden

Maria Davydova,

Department of Radiology, Memorial Sloan-Kettering Cancer Center, New York, NY 10065, USA

Dr. Nigel Lengkeek,

Australian Nuclear Science and Technology Organisation Lucas Heights, NSW 2234, Australia

Dr. Ivan Greguric,

Australian Nuclear Science and Technology Organisation Lucas Heights, NSW 2234, Australia

Dr. Michael R. Whittaker,

Department of Drug Delivery Disposition and Dynamics, Monash Institute of Pharmaceutical Sciences, Parkville, VIC 3052, Australia

Dr. John F. Quinn,

Department of Drug Delivery Disposition and Dynamics, Monash Institute of Pharmaceutical Sciences, Parkville, VIC 3052, Australia

Prof. Jonathan B. Baell,

Department of Medicinal Chemistry, Monash Institute of Pharmaceutical Sciences, Parkville, VIC 3052, Australia

Prof. Jason S. Lewis,

Department of Radiology, Memorial Sloan-Kettering Cancer Center, New York, NY 10065, USA

Prof. Thomas P. Davis

Department of Drug Delivery Disposition and Dynamics, Monash Institute of Pharmaceutical Sciences, Parkville, VIC 3052, Australia

Abstract

To improve the signal-to-noise ratio of hypoxia positron emission tomography (PET) imaging, stimuli-responsive polymers are designed for the delivery of the hypoxia PET tracer fluorine-18 labeled fluoromisonidazole ([¹⁸F]FMISO). Linear poly(*N*-(2-(hydroxypropyl)methacrylamide)) polymers are functionalized with hydrazide linkers that form pH-sensitive acyl hydrazone bonds

lewisj2@mskcc.org, thomas.p.davis@monash.edu.

Supporting Information

Supporting Information is available from the Wiley Online Library or from the author.

Conflict of Interest

The authors declare no conflict of interest.

after their conjugation to an [^{18}F]FMISO ketone analogue. The release of the [^{18}F] FMISO ketone analogue from the polymers is considerably faster at a lower pH and its uptake is significantly higher in cancer cells growing under acidic conditions. Additionally, the retention of the PET tracer is significantly higher in hypoxic cells compared to normoxic cells. The delivery of a PET tracer using stimuli-responsive polymers may be an attractive strategy to improve signal-to-noise ratios in PET imaging.

Keywords

fluoromisonidazole; hypoxia; polymers; stimuli-responsive materials

Hypoxia is the physiological phenomenon in which tissue experiences low levels of oxygen due to a compromised oxygen supply. In cancer and cardiovascular diseases, hypoxia leads to the activation of biological processes that are associated with poor patient outcome.^[1] Positron emission tomography (PET) imaging using fluorine-18 labeled fluoromisonidazole ([^{18}F]FMISO) is directly correlated to tissue oxygen levels and provides an adequate trade-off between sensitivity, specificity, imaging time, tumor penetration depth, radiation burden, and invasiveness.^[2,3] Its main disadvantages are the slow washout of the non-metabolized tracer and the high background signal in surrounding tissues.^[4] Although [^{18}F]FMISO arguably qualifies as one of the most valuable hypoxia PET tracers of the moment, its widespread (pre)clinical use is hampered by its suboptimal signal-to-noise ratio, which is due to the high background uptake. Whereas the slow washout is an intrinsic part of nitroimidazole metabolism, the signal-to-noise ratio of [^{18}F]FMISO could significantly be improved if its uptake in off-target tissues could be reduced.

To facilitate this, the delivery of [^{18}F]FMISO by nanocarriers may be a suitable strategy for preventing its diffusion through off-target cell membranes and thereby minimizing the background signal. Poly(*N*-(2-(hydroxypropyl)methacrylamide)) (p(HPMA)) has been the most widely used polymeric nanocarrier in clinical trials to date.^[5] Previously published pharmacokinetic data on linear p(HPMA) demonstrate that the majority of p(HPMA) polymers with a molecular weight of 35–40 kDa are cleared from the blood within 6–8 h after injection, matching the imageable timeframe for fluorine-18 of 3–4 half-lives.^[6] Therefore, we postulated that the use of 35–40 kDa linear p(HPMA) polymers for the delivery of [^{18}F]FMISO would considerably reduce its uptake in off-target tissues, with minimal systemic background signal remaining at the time of imaging.

In order to enable the uptake and retention of [^{18}F]FMISO in hypoxic cells, the molecule needs to be released from the polymer carrier scaffold at the target site. This can be achieved by the use of designed stimuli-responsive linkers that are cleaved in the presence of tumor microenvironment triggers, such as a decrease in pH. Hypoxia is generally accompanied by a shift from aerobic to anaerobic metabolism, which significantly lowers the intra-tumoral pH.^[7,8] In cancer, accumulation is further assisted by the increased passive delivery of the polymer-[^{18}F]FMISO complex to the tumor via the enhanced permeability and retention effect, which refers to the extensive angiogenesis, defective vascular architecture, impaired

lymphatic drainage, and increased expression of proteins affecting vascular permeability.^[9,10]

Schiff bases offer a versatile linker strategy as they hydrolyze under acidic conditions and their stability can easily be tuned by modifying the adjacent chemical structure.^[11] We and others have used Schiff bases for the delivery and release of small molecules from large nanocarrier complexes.^[12–15] In the current study, we equipped p(HPMA) with functional handles that can form labile acyl hydrazone links upon conjugation with [¹⁸F]FMISO. To investigate this strategy, we developed a ketone analogue of [¹⁸F]FMISO and examined its reversible conjugation to a functional p(HPMA) scaffold. We also demonstrated its pH-stimulated release and increased uptake and retention in cancer cells under hypoxic conditions.

Linear p(HPMA) (3) was synthesized via reversible addition fragmentation chain transfer (RAFT) polymerization (Scheme 1), with a molecular weight (MW) of 35.3 kDa and polydispersity index (PDI) of 1.31 (Figure 1A,F and Table 1). To prevent cross-reactivity of the RAFT end-group, the terminal dodecyl trithiocarbonate moiety was removed by exposing the polymer to air at 80 °C in the presence of azobis(isobutyronitrile). Successful removal of the end group chromophore and maintenance of polymer characteristics were confirmed by UV–vis and gel permeation chromatography (GPC) (Figure 1D,F; Figure S1, Supporting Information; Table 1). To allow for the functionalization of the polymer with pH-sensitive linkers via “click” chemistry, the p(HPMA) (4) was first partly functionalized with 2-bromo-2-methylpropanoate, followed by its azidation (Figure 1B,F and Table 1). The azidation was confirmed by the appearance of an azide-characteristic peak at $\approx 2100\text{ cm}^{-1}$ in the ATR–FTIR spectrum of p(HPMA-*co*-MAP) (5; Figure 1E). The functionalization was kept at 6% of the monomer units (corresponding to $\approx 10\text{ wt}\%$), since the pharmacokinetic and cytotoxic profiles of a polymer are generally retained when its degree of functionalization is kept $\leq 10\text{ wt}\%$.^[5] A Boc-protected alkyne hydrazide linker (6) was synthesized (Figures S2 and S3, Supporting Information) and subsequently reacted with the azide groups via standard copper-catalyzed click chemistry. The successful conjugation was confirmed by disappearance of the characteristic azide peak in the ATR–FTIR spectrum (Figure 1E). Boc-protection of the hydrazide linkers was required to prevent copper-mediated complexation of the polymers. Therefore, to minimize the formation of large polymer aggregates, trifluoroacetic acid (TFA)-based deprotection of the linkers was performed only directly prior to their conjugation to the [¹⁸F]FMISO ketone analogue. Still, some aggregation was observed in the final product, as demonstrated by slight peak asymmetry in the GPC trace of p(HPMA-*co*-MHP) (7; Figure 1F). The final linker-functionalized polymer p(HPMA-*co*-MHP) (7) was synthesized with a MW of 37.2 kDa and PDI of 1.27 (Figure 1C and Table 1). As such, the MW was within the targeted MW range of 35–40 kDa, thus maintaining the optimal pharmacokinetic profile for the delivery of [¹⁸F]FMISO.^[6]

A Schiff base is formed when an amine reacts with an aldehyde or a ketone. Therefore, we designed a ketone analogue of [¹⁸F]FMISO that allowed its conjugation to the hydrazide linkers on p(HPMA-*co*-MHP) (7). First, acetylated MISO ketone (10) was synthesized by reacting 2-nitroimidazole with 3-chloro-2-oxopropyl acetate under standard alkylation

conditions (Figures S4 and S5, Supporting Information). To allow for its radiofluorination, we aimed to introduce a triflate at the position of the acetyl group in 10, which is a good leaving group for nucleophilic fluorination reactions in general.^[16] However, due to the high overall reactivity of triflates, protection of the carbonyl was required to prevent intramolecular nucleophilic epoxidation. Therefore, after TFA-deprotection of 10 (Figures S6 and S7, Supporting Information), we produced 12 by ketal formation in the presence of methanol (Figures S8 and S9, Supporting Information). The precursor for radiofluorination (13) was then synthesized by triflation of its alcohol terminus (Figures S10 and S11, Supporting Information). The radiosynthesis of [¹⁸F]FMK (14) was executed in two steps, comprising the radiolabeling of 13 with ¹⁸F in acetonitrile for 15 min at 100 °C (Figure S12, Supporting Information), followed by deprotection of the ketone with hydrochloric acid for 20 min at 100 °C. The final product was obtained after preparative HPLC, yielding [¹⁸F]FMK (14) with high specific activity (1.5 GBq mg⁻¹), good radiochemical purity (>99%), and good radiochemical yield (73%) (Figure 2A). The total synthesis time was 50–60 min, calculated from the start until the end of the radiosynthesis. As such, the radiolabeling procedure followed standard operating procedures for the radiosynthesis of [¹⁸F]FMISO, involving one radiofluorination step and one deprotection step, which conveniently would allow for the large-scale, high-activity production of [¹⁸F]FMK using commercially available automated synthesis modules for [¹⁸F]FMISO.^[17] Alternative synthetic routes—such as direct oxidation of [¹⁸F]FMISO—would not be desirable, as these generally require prolonged reaction times in which the majority of ¹⁸F will undergo decay.^[18]

Generally, Schiff bases form after elimination of water from the system and in the presence of a catalyst that activates the carbonyl moiety to increase its reactivity toward the nucleophilic amines.^[19] To find the optimal conditions for the conjugation of [¹⁸F]FMK (14) to the hydrazide linkers on p(HPMA-*co*-MHP) (7), while preserving their hydrolytic propensity, we explored the use of different solvents (*N,N*-dimethylformamide, dimethylsulfoxide, methanol, acetonitrile, toluene, dichloromethane, tetrahydrofuran), drying agents (MgSO₄, molecular sieves), Brønsted–Lowry acids (TsOH, AcOH), Lewis acids (Sc(OTf)₃, B(OCH₂CF₃)₃, TTIP), bases (TEA, DIPEA), and reaction temperatures (0, 25, 60, 90, 140 °C) (Figure S13, Supporting Information). Maximum conjugation yields were obtained using TTIP as catalyst in THF at 60 °C, forming a pH-labile acyl hydrazone bond between [¹⁸F]FMK and p(HPMA-*co*-MHP). Although high conjugation yields were also achieved using Sc(OTf)₃ in DMF at 140 °C, the resulting product appeared stable to hydrolysis in an acidic environment, most likely due to the irreversible ketal formation between [¹⁸F]FMK and the alcohol groups of p(HPMA) at high temperatures. Conjugation in the presence of TTIP allowed for conjugation at lower temperatures due to its (Lewis) acidity, activating the ketone, and water scavenging properties, which contributed to the elimination of water from the reaction.^[20] The final product (p(HPMA)-[¹⁸F]FMK, 15), with a specific activity of 37 MBq mg⁻¹ and good radiochemical yield (>95%) and purity (>99%), was recovered by precipitation in a diethyl ether/hexane mixture (Figure 2B).

The released fraction of [¹⁸F]FMK from 15 at different acidity levels was measured by instant thin layer chromatography (iTLC) after dissolving the construct in aqueous buffers of pH = 8, 6, and 4 (Figure 3A). To prevent the re-conjugation of [¹⁸F]FMK to p(HPMA-*co*-

MHP) during the experiment, a large excess of butanone was added, simulating the in vivo situation in which [^{18}F]FMK and p(HPMA-*co*-MHP) are instantly separated upon hydrolysis of the linkers due to physiological processes.^[11] At pH = 8, p(HPMA)-[^{18}F]FMK (15) remained intact ($100.2 \pm 5.4\%$) for at least 60 min. At pH = 6, [^{18}F]FMK was steadily but significantly ($p < 0.01$) released from the polymer, with $93.8 \pm 3.1\%$ intact p(HPMA)-[^{18}F]FMK remaining after 60 min. At pH = 4, only $91.4 \pm 1.7\%$ of p(HPMA)-[^{18}F]FMK was intact after 60 min ($p = 0.03$). Due to the radioactive decay of ^{18}F below the detection limit of the iTLC equipment at later timepoints, measurement data were extrapolated using an exponential model to estimate the release rates up to 4 h.^[11] These measurements supported our hypothesis that [^{18}F]FMK was released from p(HPMA)-[^{18}F]FMK under acidic conditions due to hydrolysis of the pH-sensitive linkers, with a faster release at a lower pH.

To confirm these data in vitro, proof-of-concept was provided by measuring the uptake of [^{18}F]FMK in SQ20b laryngeal squamous cell carcinoma cells. SQ20b cells were selected for these experiments due to their high sensitivity toward hypoxic stimuli.^[21] To simulate pH changes in the tumor microenvironment, cells were incubated in culture media with either pH = 7.4 or 5.0. Furthermore, to compare uptake between hypoxic and normoxic cells, incubation was performed in either a hypoxia chamber at 1% O_2 or a standard cell incubator at 18.5% O_2 . Under hypoxic conditions, the uptake per cell after 4 h was significantly higher ($p < 0.01$) for cells incubated at pH = 5.0 ($11 \pm 0.6 \times 10^{-3}$ counts per cell) compared to uptake at pH = 7.4 ($8 \pm 1 \times 10^{-3}$ counts per cell) (Figure 3B). These data imply that hydrolysis of the pH-sensitive linkers was indeed faster at a lower pH, thereby releasing higher amounts of [^{18}F]FMK, which is subsequently taken up by the cells. Furthermore, cells in a hypoxic environment ($11 \pm 0.6 \times 10^{-3}$ counts per cell) demonstrated a higher overall uptake ($p < 0.01$) than cells under normoxic conditions ($8 \pm 0.2 \times 10^{-3}$ counts per cell) at the same pH (pH = 5.0) (Figure 3C), suggesting that the hypoxia-targeting properties of [^{18}F]FMISO were retained within the (released) ketone analogue ([^{18}F]FMK). These data were confirmed in control experiments with free (unconjugated) [^{18}F]FMK ($36 \pm 9 \times 10^{-3}$ counts per cell at pH = 5.0; $27 \pm 0.6 \times 10^{-3}$ counts per cell at pH = 7.4) and [^{18}F]FMISO ($34 \pm 2 \times 10^{-3}$ counts per cell at pH = 5.0; $26 \pm 8 \times 10^{-3}$ counts per cell at pH = 7.4), which demonstrated a similar uptake in SQ20b cells under hypoxic conditions (Figure S14, Supporting Information). These control experiments suggest that the pharmacokinetic behavior of the daughter compound ([^{18}F]FMK) is similar to that of the original molecule ([^{18}F]FMISO). Moreover, these data confirm that the polymer hampers the overall cellular uptake of [^{18}F]FMK. That is, the uptake of free [^{18}F]FMK after 4 h under hypoxic conditions (Figure S14A, Supporting Information) was 3.3 to 3.4 times higher ($p < 0.01$) than the uptake of the conjugated products (Figure 3B). This suggests that cellular uptake is indeed largely prevented by complexation to the polymer. Although the uptake of free [^{18}F]FMK and free [^{18}F]FMISO was somewhat higher at pH = 5.0 than at pH = 7.4, the observed differences were not statistically significant ($p = 0.11$ and 0.09 , respectively), indicating that the pH does not substantially affect the uptake of the tracer itself. To confirm that cell viability was not affected by changes in pH, we compared the viability at pH = 7.4 and 5.0. No significant differences were observed at the time of the experiment ($p = 0.55$; Figure S15A, Supporting Information). Similarly, no significant viability differences were

measured between cells growing in hypoxic and normoxic conditions ($p = 0.91$; Figure S15B, Supporting Information).

The level of acidity in the hypoxic extracellular environment is debated. Whereas the general assumption is that the pH of the tumor microenvironment is 5.7–7.8 for most solid tumors, it is also well-known that hypoxia may further decrease the extracellular pH.^[22,23] The complexity of physiological processes involved in hypoxia makes the real extracellular pH difficult to predict. Our in vitro experiments provide a proof-of-concept for the pH-stimulated delivery of an [¹⁸F]FMISO analogue using p(HPMA) and its subsequent increased intracellular uptake, warranting further investigation in in vivo models. Generally, PET imaging is preferred within three half-lives after the injection of the tracer, although higher administered doses or longer image acquisition times may substantially extend waiting times. In vivo optimization will be required to find the ideal trade-off between signal intensity and the release and cellular uptake of [¹⁸F]FMK, and to allow for PET imaging at later timepoints (e.g., 6–8 h).

Linear p(HPMA) was functionalized with pH-sensitive linkers for the delivery of [¹⁸F]FMK, a novel [¹⁸F]FMISO analogue, into the hypoxic microenvironment. Release of the tracer was significantly faster at lower pH and its cellular uptake was significantly higher in hypoxic cells and under acidic conditions. Together, our data suggest that the delivery of [¹⁸F]FMK by p(HPMA) polymers is a promising new approach to ultimately improve the signal-to-noise ratio of hypoxia PET imaging based on [¹⁸F]FMISO.

Supplementary Material

Refer to Web version on PubMed Central for supplementary material.

Acknowledgements

Funding from Australian Research Council (ARC) Centre of Excellence in Convergent Bio-Nano Science and Technology (CE140100036) and NIH Cancer Center Support Grant P30 CA008748-48, supporting MSK Small Animal Imaging Core, Radiation Core, and Research Animal Resource Facilities are gratefully acknowledged. J.S.L. kindly acknowledges Mr. William H. and Mrs. Alice Goodwin and the Commonwealth Foundation for Cancer Research and the Center for Experimental Therapeutics of Memorial Sloan Kettering Cancer Center, and NIH grant R35 CA232130.

References

- [1]. Michiels C, Am. J. Pathol 2004, 164, 1875. [PubMed: 15161623]
- [2]. Lopci E, Grassi I, Chiti A, Nanni C, Cicoria G, Toschi L, Fonti C, Lodi F, Mattioli S, Fanti S, Am. J. Nucl. Med. Mol. Imaging 2014, 4, 365. [PubMed: 24982822]
- [3]. Bell C, Dowson N, Fay M, Thomas P, Puttick S, Gal Y, Rose S, Semin. Nucl. Med 2015, 45, 136. [PubMed: 25704386]
- [4]. Dunphy MP, Lewis JS, J. Nucl. Med 2009, 50, 106S. [PubMed: 19380404]
- [5]. Duncan R, Nat. Rev. Cancer 2006, 6, 688. [PubMed: 16900224]
- [6]. Etrych T, Subr V, Strohalm J, Sirova M, Rihova B, Ulbrich K, J. Controlled Release 2012, 164, 346.
- [7]. Wike-Hooley JL, Haveman J, Reinhold HS, Radiother. Oncol 1984, 2, 343. [PubMed: 6097949]
- [8]. Wei X, Chen X, Ying M, Lu W, Acta Pharm. Sin. B 2014, 4, 193. [PubMed: 26579383]
- [9]. Maeda H, Wu J, Sawa T, Matsumura Y, Hori K, J. Controlled Release 2000, 65, 271.

- [10]. Kobayashi H, Watanabe R, Choyke PL, *Theranostics* 2013, 4, 81. [PubMed: 24396516]
- [11]. Kalia J, Raines RT, *Angew. Chem., Int. Ed* 2008, 47, 7523.
- [12]. Jackson AW, Fulton DA, *Polym. Chem* 2013, 4, 31.
- [13]. Karagoz B, Esser L, Duong HT, Basuki JS, Boyer C, Davis TP, *Polym. Chem* 2014, 5, 350.
- [14]. Li Y, Duong HTT, Laurent S, MacMillan A, Whan RM, Elst LV, Muller RN, Hu J, Lowe A, Boyer C, Davis TP, *Adv. Healthcare Mater* 2015, 4, 148.
- [15]. Kamaly N, Yameen B, Wu J, Farokhzad OC, *Chem. Rev* 2016, 116, 2602. [PubMed: 26854975]
- [16]. Kim K-Y, Kim BC, Lee HB, Shin H, *J. Org. Chem* 2008, 73, 8106. [PubMed: 18808183]
- [17]. Wang M, Zhang Y, Zhang Y, Yuan H, *J. Radioanal. Nucl. Chem* 2009, 280, 149.
- [18]. Grunbaum Z, Freauff SJ, Krohn KA, Wilbur DS, Magee S, Rasey JS, *J. Nucl. Med* 1987, 28, 68. [PubMed: 3794812]
- [19]. da Silva CM, da Silva DL, Modolo LV, Alves RB, de Resende MA, Martins CVB, de Fátima Â, *J. Adv. Res* 2011, 2, 1.
- [20]. Salmi C, Letourneux Y, Brunel JM, *Lett. Org. Chem* 2006, 3, 396.
- [21]. Carlin S, Zhang H, Reese M, Ramos NN, Chen Q, Ricketts S-A, *J. Nucl. Med* 2014, 55, 515. [PubMed: 24491409]
- [22]. Lee ES, Gao Z, Bae YH, *J. Controlled Release* 2008, 132, 164.
- [23]. Kato Y, Ozawa S, Miyamoto C, Maehata Y, Suzuki A, Maeda T, Baba Y, *Cancer Cell Int.* 2013, 13, 89. [PubMed: 24004445]

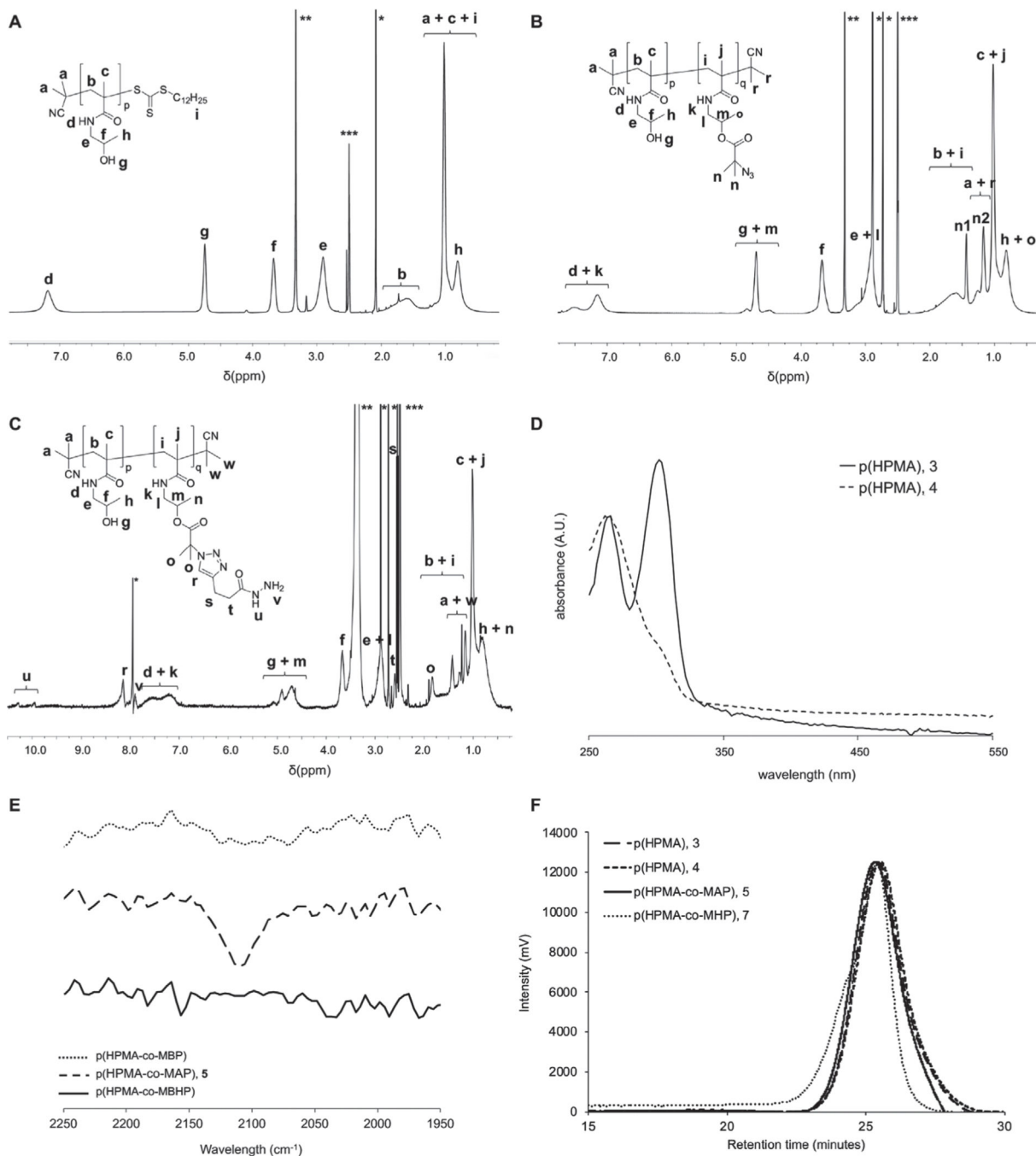


Figure 1. ^1H NMR spectra in $\text{DMSO}-d_6$ of A) p(HPMA), B) p(HPMA-*co*-MAP), and C) p(HPMA-*co*-MHP) (*acetone (A) or DMF (B,C), **water, ***DMSO). D) UV-vis spectrum, showing significant signal reduction at 310 nm, which indicates that the RAFT end-group was removed. E) ATR-FTIR spectra of p(HPMA-*co*-MBP), p(HPMA-*co*-MAP), and p(HPMA-*co*-MBHP), demonstrating the appearance in p(HPMA-*co*-MAP) and disappearance in p(HPMA-*co*-MBHP) of an azide peak at $\approx 2100\text{ cm}^{-1}$, indicating that the functionalization

with the hydrazide linker was successful. F) GPC traces of p(HPMA) (3), p(HPMA) (4), p(HPMA-*co*-MAP) (5), and p(HPMA-*co*-MHP) (7).

Author Manuscript

Author Manuscript

Author Manuscript

Author Manuscript

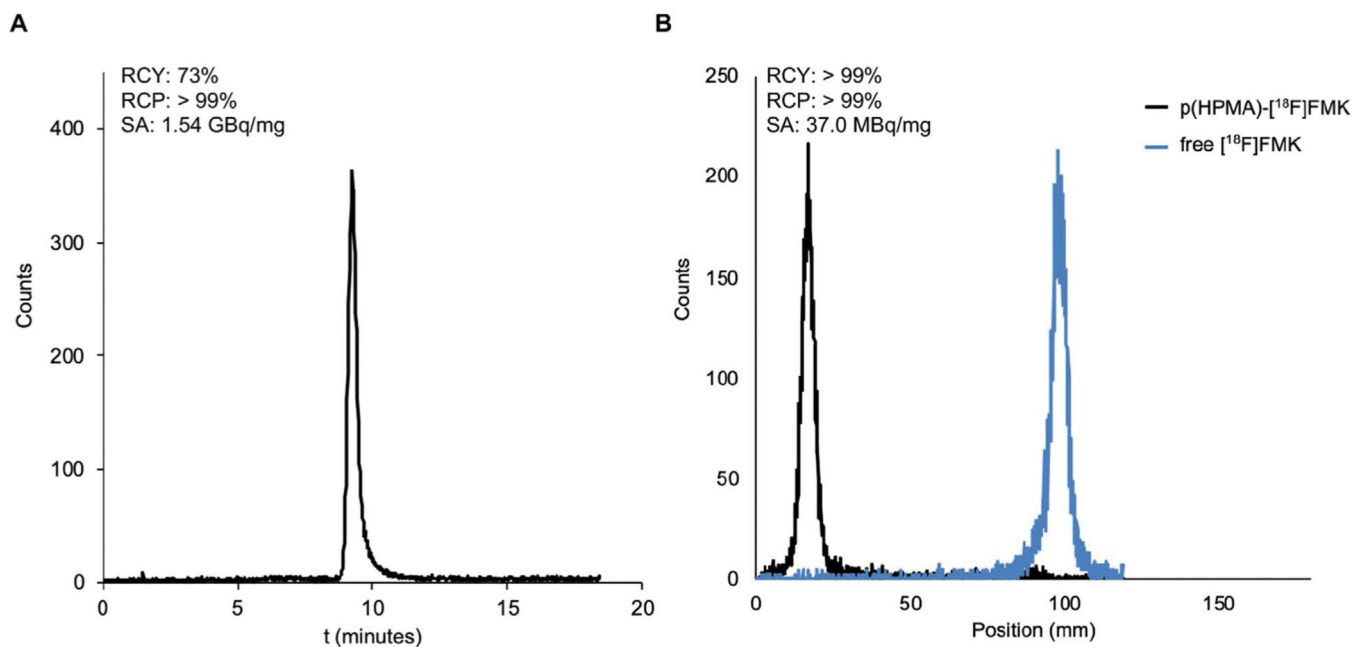


Figure 2.

A) Radio-HPLC chromatogram of purified [^{18}F]FMISO ketone (14). B) iTLC chromatograms of p(HPMA)-[^{18}F]FMK (15) and non-conjugated [^{18}F]FMK (14).

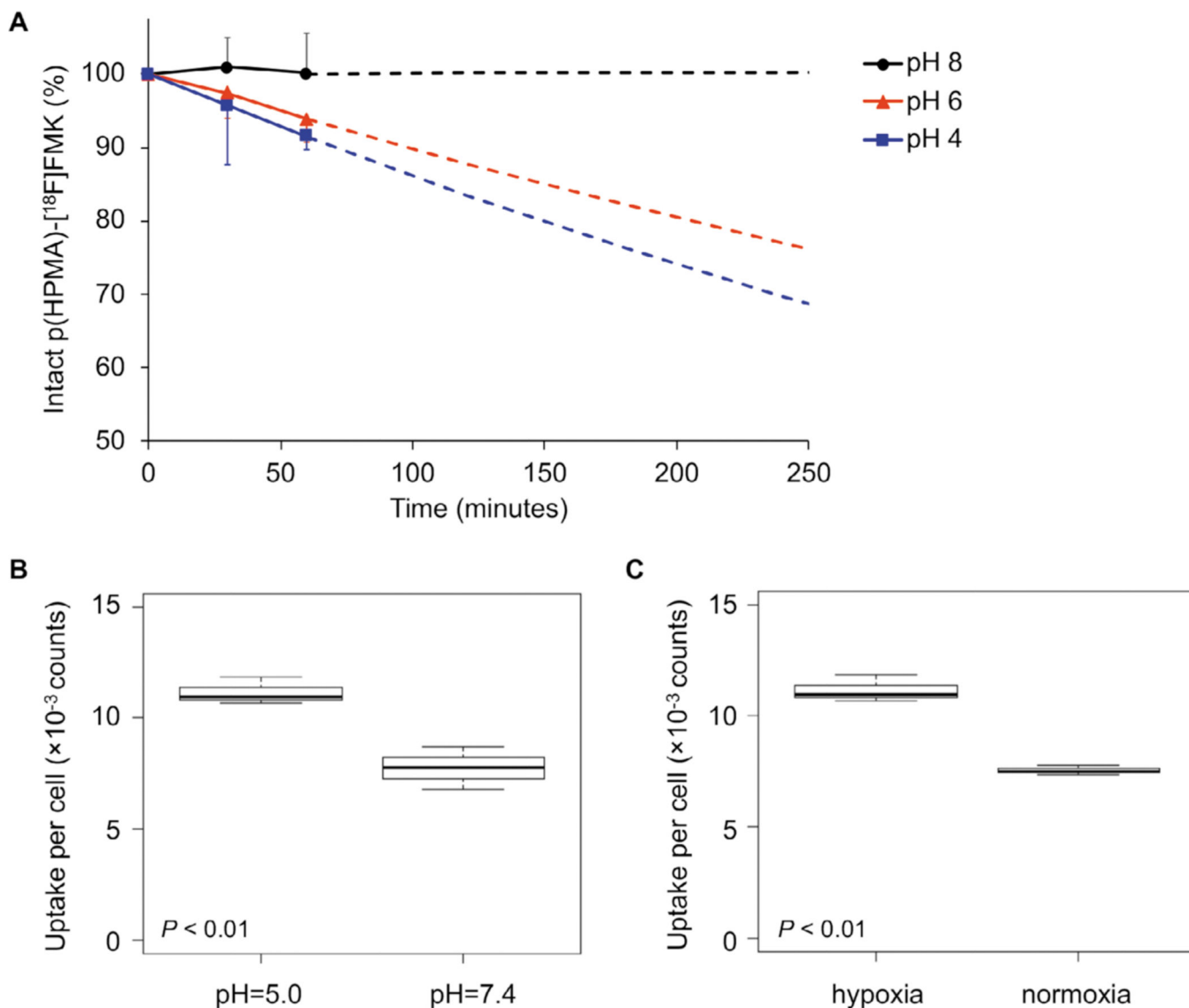
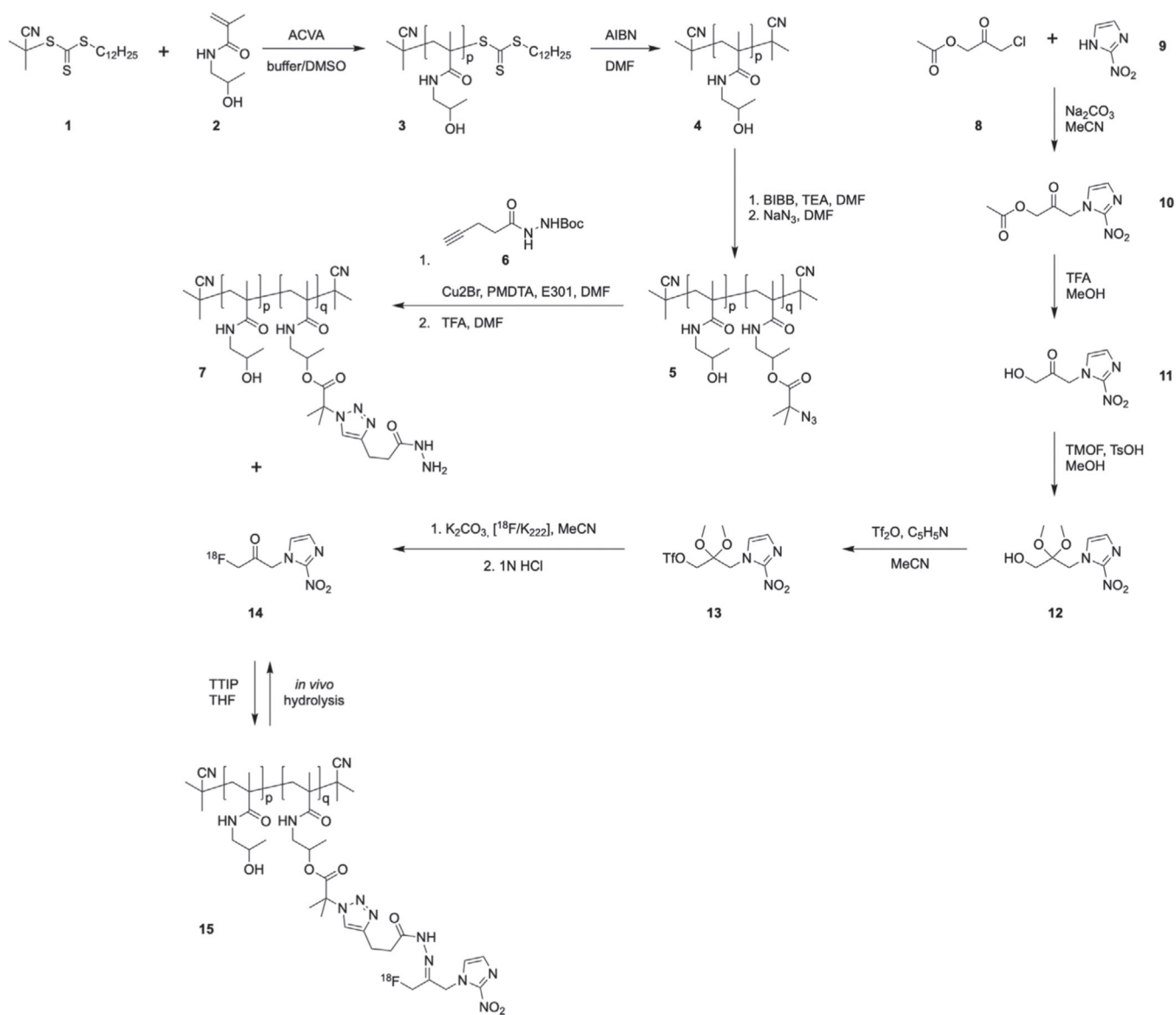


Figure 3.

A) Release studies of p(HPMA)-[^{18}F]FMK (15) in aqueous buffer at pH = 4, 6, and 8. In slightly basic conditions (pH = 8), the pH-sensitive linker was not hydrolyzed, preventing the release of [^{18}F]FMK from the p(HPMA) polymers. In acidic conditions, [^{18}F]FMK was readily released from the p(HPMA) polymers ($p < 0.01$ for pH = 6 and $p = 0.03$ for pH = 4). Measurement data were extrapolated up to the in vitro evaluation time point in SQ20b cells (4 h) based on an exponential model (dotted lines). B,C) In vitro uptake in human SQ20B head and neck carcinoma cells after 4 h incubation. B) The uptake per cell was significantly higher at pH = 5 compared to pH = 7 ($p < 0.01$). C) The uptake per cell was significantly higher in hypoxic cells compared to normoxic cells ($p < 0.01$).

**Scheme 1.**

Schematic representation of the radiosynthesis of [¹⁸F]FMK and its conjugation to p(HPMA). [¹⁸F]FMK is released from the polymer after hydrolysis of the acyl hydrazone linkers under acidic conditions.

Table 1.

Characterization of the (functionalized) p(HPMA) polymers.

| Compound | DP ^{a)} | No. of functionalized units [%] | MW ^{b)} [kDa] | PDI ^{c)} | |
|-----------------|------------------|---------------------------------|------------------------|-------------------|------|
| p(HPMA) | 3 | 244 | 0 (0) | 35.3 | 1.31 |
| p(HPMA) | 4 | 244 | 0 (0) | 35.1 | 1.29 |
| p(HPMA-co-MBP) | - | 244 | 14 (6) | 37.2 | 1.26 |
| p(HPMA-co-MAF) | 5 | 244 | 14 (6) | 37.2 | 1.27 |
| p(HPMA-co-MBHP) | - | 244 | 14 (6) | 37.2 | 1.27 |
| p(HPMA-co-MHP) | 7 | 244 | 14 (6) | 37.2 | 1.27 |

^{a)}DP, degree of polymerisation;

^{b)}MW, molecular weight, based on ¹H NMR;

^{c)}PDI, polydispersity index.